

Article

# A novel method for glucose detection using dual-modal carbon dots for colorimetric and ratiometric fluorescence analysis

Chunling Yuan, Xiaotiao Yao, Yuanjin Xu, Xiu Qin, Rui Shi, Shiqi Cheng, Yilin Wang\*

Guangxi Key Laboratory of Electrochemical Energy Materials, School of Chemistry and Chemical Engineering, Guangxi University, Nanning 530004, China

\* Corresponding author: Yilin Wang, [theanalyst@163.com](mailto:theanalyst@163.com)

## CITATION

Yuan C, Yao X, Xu Y, et al. A novel method for glucose detection using dual-modal carbon dots for colorimetric and ratiometric fluorescence analysis. *Advances in Analytic Science*. 2024; 5(1): 2043. <https://doi.org/10.54517/aas.v5i1.2043>

## ARTICLE INFO

Received: 5 March 2024

Accepted: 12 April 2024

Available online: 1 May 2024

## COPYRIGHT



Copyright © 2024 by author(s). *Advances in Analytic Science* is published by Asia Pacific Academy of Science Pte. Ltd. This work is licensed under the Creative Commons Attribution (CC BY) license. <https://creativecommons.org/licenses/by/4.0/>

**Abstract:** Iron-based nitrogen co-doped carbon dots (Fe, N-CDs) were synthesized from taro leaf biomass via a hydrothermal process using ammonium ferric sulfate dodecahydrate and urea. The synthesized Fe, N-CDs exhibited peroxidase-like activity and strong fluorescence at 450 nm. A dual-mode colorimetric/ratiometric fluorescence assay for hydrogen peroxide (H<sub>2</sub>O<sub>2</sub>) detection was developed using Fe, N-CDs and o-phenylenediamine (OPD) as probes. In the presence of H<sub>2</sub>O<sub>2</sub>, OPD was oxidized to 2,3-diaminophenazine (DAP), which is yellow and absorbs at 420 nm. Under 360 nm excitation, DAP emits fluorescence at 550 nm and quenches the fluorescence of Fe, N-CDs at 450 nm due to the internal fluorescence filtering effect. This enables the quantitative analysis of H<sub>2</sub>O<sub>2</sub> using the absorbance at 420 nm (*A*<sub>420</sub>) and the fluorescence intensity ratio of DAP to Fe, N-CDs (*I*<sub>550</sub>/*I*<sub>450</sub>). Since glucose oxidase can convert glucose to H<sub>2</sub>O<sub>2</sub>, the assay was extended to glucose determination. At pH 5.4, 40 °C, with 1.75 mmol/L OPD and a 25-minute reaction time, the method showed a linear relationship between the *A*<sub>420</sub> and *I*<sub>550</sub>/*I*<sub>450</sub> values and glucose concentration in the range of 1.0~100 μmol/L, with detection limits of 0.8 μmol/L (colorimetry) and 0.6 μmol/L (ratiometry). The method was validated for glucose detection in human serum.

**Keywords:** carbon point; colorimetry; ratio fluorescence; glucose; determination

Glucose is the main energy source and metabolic intermediate in biological activities, and plays an important role in the process of life. Abnormal blood glucose level is usually considered to be related to diabetes. Hypoglycemia, metabolic disorders and other diseases [1,2]. Therefore, rapid and accurate determination of glucose concentration in serum is of great significance for disease diagnosis. At present, chromatographic analysis [3,4]. Detection techniques such as electrical analysis [5,6] and optical analysis [7,8] have been applied to the determination of glucose. Because of its fast response. With the advantages of low cost and high sensitivity, colorimetric and fluorescent light analysis techniques have attracted much attention [7]. With the continuous development of nanotechnology, various nano materials have been widely used in the field of optical analysis. Some metal oxides [9], metal sulfide [10] and noble metal [11] nano materials are used for colorimetric determination of glucose because they have peroxidase like properties and can catalyze the oxidation of 3,3',5,5'-tetramethylbenzidine (TMB) by H<sub>2</sub>O<sub>2</sub>. Due to the large absorption spectrum bandwidth and molar absorption coefficient, mno<sub>2</sub> nanosheets can effectively quench rare earth nanoparticles (NaYF<sub>4</sub>:YB, Tm@NaYF<sub>4</sub>) The fluorescence of nanoparticles [12] and copper nanoclusters [13]; the addition of H<sub>2</sub>O<sub>2</sub> can reduce MnO<sub>2</sub> to Mn and restore the quenched fluorescence. Combined with the principle that glucose oxidase catalyzes the oxidation of glucose to H<sub>2</sub>O<sub>2</sub>,

the above nano materials have been used to construct “off-on” fluorescent probes for the determination of glucose concentration. So far, there are many reports on the determination of glucose by colorimetry or fluorescence, but few reports on the simultaneous determination of glucose by these two methods [14,15]. Studies [14,15] showed that  $\text{ZnFe}_2\text{O}_4$  magnetic microspheres. Pd nanoparticles can catalyze the oxidation of o-phenylenediamine (OPD) by  $\text{H}_2\text{O}_2$  to produce fluorescent yellow product 2,3-diaminophenazine (DAP); the presence of DAP will lead to boron and nitrogen Co doped carbon dots (B, N-CDs). Fluorescence quenching of  $\text{C}_3\text{N}_4$  nanosheets. Accordingly, Li [14] and Qiu [15] research groups have developed a new dual signal glucose determination method based on colorimetry and ratio fluorescence, both of which use two nano (or micron) materials.

Compared with other nano materials, CDs has the advantages of simple preparation. High stability. Good biocompatibility and strong luminous ability [16]. As peroxidase like or fluorescent nano materials, CDs are widely used in biochemical analysis, cell imaging and other research fields [17–22], but there are few reports of bifunctional CDs with peroxidase like activity and fluorescence emission characteristics [23–25]. CDs prepared from biomass materials such as *Azadirachta indica* leaves [23] and mustard seeds [24] can not only emit fluorescence, but also catalyze the oxidation of TMB by  $\text{H}_2\text{O}_2$ . However, relevant studies only apply its catalytic function to the determination of  $\text{H}_2\text{O}_2$  and ascorbic acid; bifunctional iron can be prepared by using organic amine and ferric nitrate as reactants. Nitrogen Co doped CDs, which can be used for colorimetric/ratio fluorescence determination of xanthine [25]. Element doping can not only improve the fluorescence quantum yield of CDs, but also change the internal electronic environment of CDs, endow CDs with new functions and expand its application fields [26]. Based on the key role of iron in peroxidase and the fact that nitrogen doping can improve the fluorescence characteristics of CDs, this paper takes biomass (taro leaf). Iron was prepared by hydrothermal method with ammonium ferric sulfate dodecahydrate and urea as starting materials. Nitrogen Co doped cds (Fe, N-CDs), the obtained Fe, N-CDs not only has peroxidase like activity, but also can produce strong fluorescence emission at 450 nm (**Figure 1**). Based on the bifunctional properties of Fe, N-CDs, a colorimetric/ratio fluorescence method for the determination of glucose concentration was established and successfully applied to the analysis of actual samples.

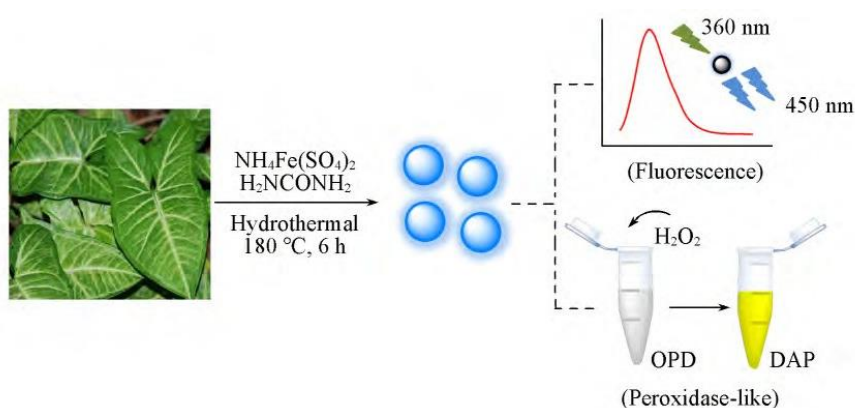


**Figure 1.** Preparation and properties of Fe, N-CDs.

## 1. Experimental part

### 1.1. Reagents and instruments

Ammonium ferric sulfate dodecahydrate [ $\text{NH}_4\text{Fe}(\text{SO}_4)_2 \cdot 12\text{H}_2\text{O}$ ]. Urea ( $\text{n}_2\text{hconh}_2$ ). Sodium acetate trihydrate. Glacial acetic acid and hydrogen peroxide (Guangdong Guanghua Technology Co., Ltd.); glucose. Phenylalanine. Glycine. Isoleucine. Threonine. Aspartic acid. Valine. Tryptophan and serine (Tianjin Damao Chemical Reagent Factory); O-phenylenediamine (OPD, Shanghai Aladdin Reagent Co., Ltd.); glucose oxidase (Beijing sulaibao Technology Co., Ltd.). All reagents used are analytically pure, and the experimental water is deionized water.

RF-5301PC fluorescence spectrophotometer (Shimadzu company of Japan);  $\text{uv}^{-4802}$  UV visible spectrophotometer (Shanghai longnico company); TECNAI G2 F20 S-Twin transmission electron microscope (Fei company of the United States); Nicolet IS5 Fourier transform infrared spectrometer (Thermo Fisher, USA); FLS1000 fluorescence spectrometer (Edinburgh company, UK).

### 1.2. Preparation of Fe, N-CDs

Wash the taro leaves, dry the wet water on the surface, and then cut them into pieces. Weigh 2.0 g and put them in a 75 mL reactor. Add 0.8 g  $\text{NH}_4\text{Fe}(\text{SO}_4)_2 \cdot 12\text{H}_2\text{O}$ , 0.2 g  $\text{N}_2\text{HCONH}_2$  and 25 mL deionized water, mix them evenly and seal them; place the reaction kettle in a 180 °C constant temperature drying oven for 6 h. After natural cooling to room temperature, filter with funnel to obtain dark brown solution; reuse 0.22  $\mu\text{m}$  microfiltration membrane removes large particle aggregates in the solution; dialysis the reaction solution for 24 h to remove unreacted reagents, collect the solution in the bag and dilute it to 25 mL, and store it in a 4 °C refrigerator for standby.

### 1.3. Determination of $\text{H}_2\text{O}_2$ and glucose

Determination of  $\text{H}_2\text{O}_2$ : add 0.5 mL of  $\text{H}_2\text{O}_2$  solutions with different concentrations into a series of colorimetric tubes. 0.5 mL of 17.5 mmol/L OPD solution and 100  $\mu\text{L}$  Fe, N-CDs solution, after mixing evenly, dilute to 5.0 mL with HAC NaAc (0.2 mol/L) buffer solution with pH = 5.4, and place it in a 40 °C water bath for 25 min. The absorption spectra were scanned in the range of 330~550 nm, and the fluorescence spectra were recorded under the excitation of 360 nm wavelength light. The experiments were carried out in parallel for 3 times.

Determination of glucose: add 0.5 mL of 10 mmol/L  $\text{NaH}_2\text{PO}_4\text{-Na}_2\text{HPO}_4$  (4 pH = 7.0) buffer solution successively into a series of colorimetric tubes. 0.5 mL of glucose solution with different concentrations and 0.1 mL of 2.0 mg/mL glucose oxidase were mixed evenly and incubated in a 37 °C water bath for 30 min to produce  $\text{H}_2\text{O}_2$ ; then, add 0.5 mL of 17.5 mmol/L OPD solution and 100  $\mu\text{L}$  Fe, N-CDs solution, dilute to 5.0 mL with 0.2 mol/L HAC-NAAC buffer solution (pH = 5.4), mix evenly, and the subsequent process is the same as the determination of  $\text{H}_2\text{O}_2$ . The experiment is carried out in parallel for 3 times.

## 2. Results and discussion

### 2.1. Characterization of Fe, N-CDs

The morphology and particle size of Fe, N-CDs were characterized by transmission electron microscope (TEM). It can be seen from **Figure 2A** that Fe and N-CDs are approximately spherical and have good dispersion; clear lattice stripes with a spacing of 0.23 nm can be seen from the high-resolution transmission electron microscope photos (illustration), which correspond to the graphene (100) surface [27]. According to the analysis of nano measurer software (**Figure 2B**), the particle size of Fe and N-CDs is mainly distributed in the range of 1.34~3.68 nm, and the average particle size is about 2.51 nm.

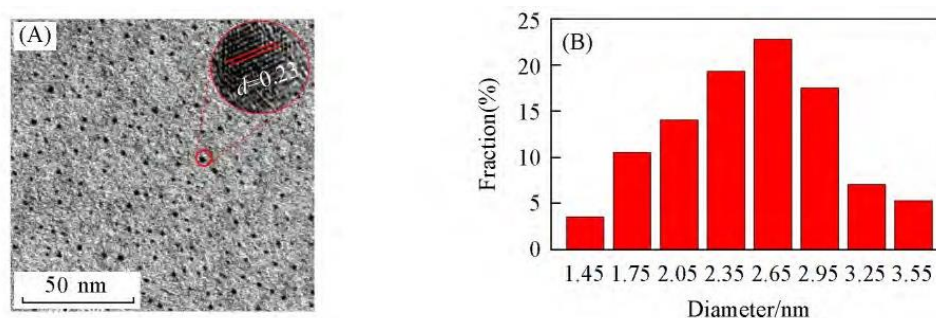


**Figure 2.** (A) TEM image; (B) particle size distribution diagram of Fe, N-CDs inset of (A) is the relative HRTEM image.

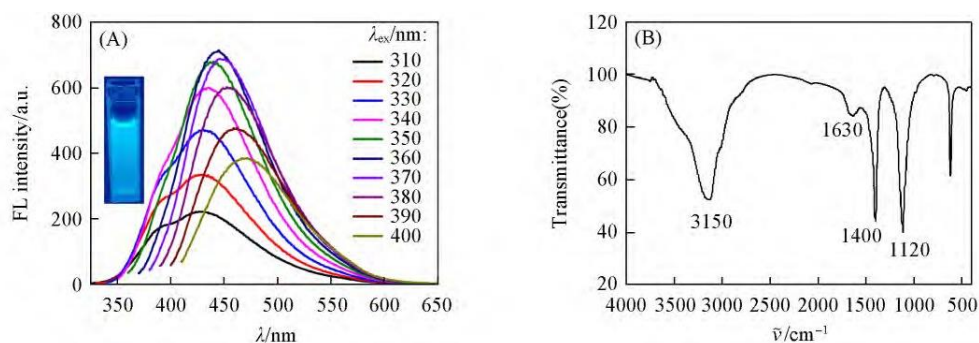


**Figure 3.** (A) Emission spectra of Fe, N-CDs excited at 310–440 nm; (B) FTIR spectrum of Fe, N-CDs.

Under the irradiation of 365 nm UV lamp, Fe, N-CDs emit bright blue fluorescence (**Figure 3A** illustration). When the excitation wavelength increased from 310 nm to 440 nm, the fluorescence emission peak of Fe, N-CDs red shifted from 427 nm to 472 nm; the fluorescence intensity increased first and then decreased; when excited by light with a wavelength of 360 nm, the fluorescence emission is the strongest (**Figure 3A**). This excitation dependent emission behavior is related to the surface defects and particle size of particles [27] Fe, N-CDs solution has strong light absorption in the UV region, and the absorption peak at 270 nm is attributed to the  $\pi$ - $\pi^*$  transition of C=C or C=N [28] (see supporting information **Figure A1** in Appendix). Fourier transform infrared spectroscopy (FTIR) was used to analyze the groups contained in Fe, N-CDs (**Figure 3B**). The wide peak at 3150

$\text{cm}^{-1}$  was attributed to the stretching vibration of O–H and N–H, the peak at  $1630\text{ cm}^{-1}$  was attributed to the stretching vibration of C=O and C=C, and the peak at  $1400$  and  $1120\text{ cm}^{-1}$  was attributed to the stretching vibration of C–OH and C–O–C, respectively. FTIR analysis showed that there were hydrophilic groups –COOH, –OH and –NH<sub>2</sub> on the surface of Fe, N-CDs, which made them have good water solubility.

The elemental composition and functional groups of Fe and N-CDs were characterized by X-ray photoelectron spectroscopy (XPS). It can be seen from the full scan spectrum (**Figure 4**) that CDs is mainly composed of carbon (44.02%), Nitrogen (13.41%), The binding energies of oxygen (39.98%) and iron (2.59%) are 284.8, 401.3, 531.5 and 710.7 EV, respectively. The high-resolution XPS spectrum of C<sub>1s</sub> contains three peaks of 284.7, 286.1 and 288.3 EV, corresponding to C=C, C=O and O–C=O<sup>1</sup> functional groups respectively [29]. The high-resolution XPS spectrum of N<sub>1s</sub> shows two peaks of 399.8 and 401.5 EV, corresponding to C–N–C and N–H functional groups respectively [30]. There are 531.3 and 532.4 Ev 2 peaks in the high-resolution XPS spectrum of O<sub>1s</sub>, which belong to C–OH/C–O–C and C=O bond respectively [31]. The Fe<sub>2p</sub> spectrum contains four peaks of 710.7, 714.1, 724.7 and 727.6 EV, corresponding to Fe<sub>2p<sub>3/2</sub></sub><sup>2+</sup>, Fe<sub>2p<sub>3/2</sub></sub><sup>3+</sup>, Fe<sub>2p<sub>1/2</sub></sub><sup>2+</sup> and Fe<sub>2p<sub>1/2</sub></sub><sup>3+</sup> [32] respectively. [See the supporting information **Figure A2A–D**]. The above results show that Fe and n elements have indeed been doped into CDs; the surface of Fe, N-CDs is rich in O-containing and N-containing functional groups.

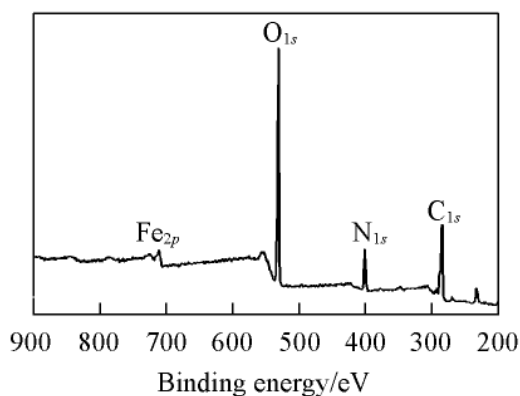


**Figure 4.** Survey spectrum of Fe, N-CDs.

## 2.2. Catalytic activity of Fe, N-CDs and mechanism of glucose double signal determination

In order to study the peroxidase like activity of Fe, N-CDs, a control experiment was carried out in HAC NaAc buffer solution with pH = 5.4. The solution containing Fe, N-CDs and OPD is colorless, and there is no absorption peak in the UV Vis Spectrum (**Figure 5A** line a); the solution containing H<sub>2</sub>O<sub>2</sub> and OPD has a weak absorption peak at 420 nm (**Figure 5A** spectral line b), and its solution is light yellow, indicating that H<sub>2</sub>O<sub>2</sub> can slowly oxidize OPD to DAP; when Fe and N-CDs are present, the solution containing H<sub>2</sub>O<sub>2</sub> and OPD has a strong absorption peak at 420 nm (**Figure 5A** spectral line c), and its solution is dark yellow. The above data show that Fe, N-CDs have peroxidase like activity and can catalyze the oxidation of

OPD by  $\text{H}_2\text{O}_2$ .

DAP solution is yellow, and its absorption peak is at 420 nm; under the excitation of 360 nm wavelength light, the fluorescence emission peak of Fe, N-CDs is located at 450 nm. It can be seen from **Figure 5B** that the absorption spectrum of DAP overlaps greatly with the fluorescence spectrum of Fe and N-CDs; when the two coexist, the fluorescence quenching of Fe, N-CDs can be caused by fluorescence internal filtration effect (IFE) or fluorescence resonance energy transfer (Fret). Before and after the addition of Fe, N-CDs, the position and absorption intensity of DAP absorption peak are almost unchanged [see the supporting information **Figure A3A**], indicating that there is no complex between Fe, N-CDs and DAP, that is, FRET between Fe, N-CDs and DAP is impossible [33]. In addition, before and after adding DAP, the fluorescence lifetime of Fe, N-CDs did not change significantly [see the supporting information **Figure A3B**], indicating that there was no charge transfer between Fe, N-CDs and DAP, so the fluorescence quenching of Fe, N-CDs was not caused by charge transfer [14]. Therefore, when the two coexist, the fluorescence quenching of Fe, N-CDs is caused by IFE.

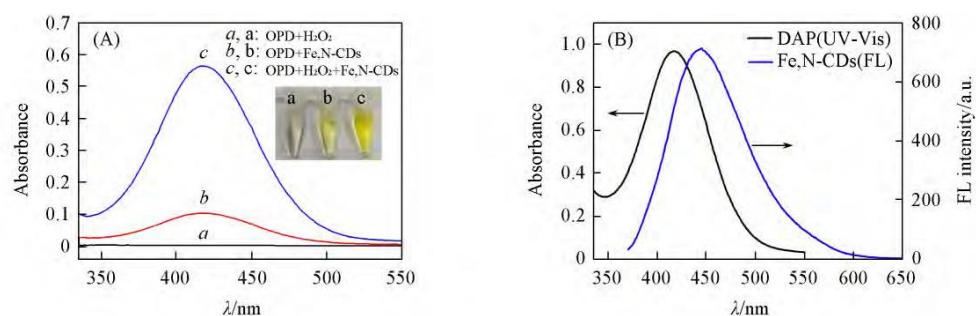


**Figure 5.** (A) Absorbance spectra of different solutions in 0.2 mol/L HAC-NaAc buffer solution at pH = 5.4; (B) absorbance spectrum of DAP and emission spectrum of Fe, N-CDs.

Fe, N-CDs can catalyze  $\text{H}_2\text{O}_2$  to oxidize OPD to produce DAP; excited by 360nm wavelength light, DAP has a fluorescence emission peak at 550 nm, while Fe, N-CDs also have a fluorescence emission peak at 450 nm under the excitation of the same wavelength light; DAP quenches the fluorescence of Fe, N-CDs through IFE. That is, adding  $\text{H}_2\text{O}_2$  to Fe, N-CDs/opd system will not only change the color of the solution, but also change the relative fluorescence intensity of DAP and Fe, N-CDs; with the increase of  $\text{H}_2\text{O}_2$  concentration, the absorbance of DAP at 420 nm and the fluorescence intensity at 550 nm increased, while the fluorescence intensity of Fe and N-CDs at 450 nm decreased. The concentration of  $\text{H}_2\text{O}_2$  can be determined by measuring the absorbance of DAP at 420 nm and the fluorescence intensity ratio of DAP to Fe, N-CDs ( $I_{550}/I_{450}$ );  $\text{H}_2\text{O}_2$  is one of the products of glucose oxidation catalyzed by glucose oxidase. Based on this, a colorimetric/ratio fluorescence dual signal glucose determination method can be further established (**Figure 6**).



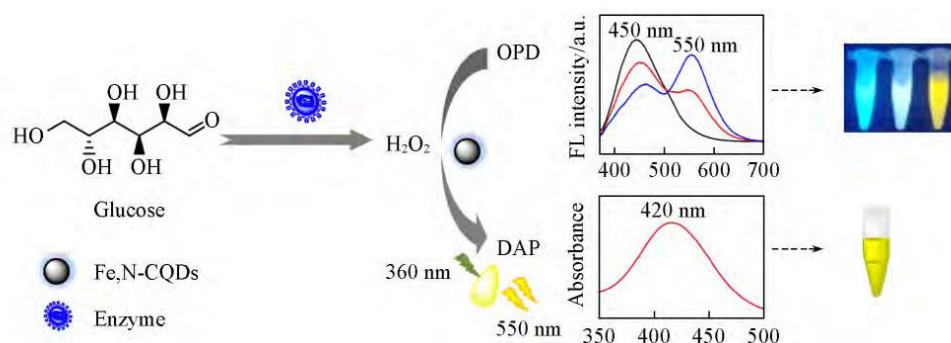


**Figure 6.** Schematic diagram of detection principle.

### 2.3. Optimization of experimental conditions

In order to obtain the best signal response, pH was investigated with the relative fluorescence intensity  $I_{550}/I_{450}$  (where  $I_{550}$  and  $I_{450}$  represent the fluorescence emission intensity at 550 and 450 nm, respectively). Temperature. Effects of reaction time and OPD concentration on the oxidation of OPD by  $H_2O_2$  catalyzed by Fe, N-CQDs. Considering that peroxidase like enzymes usually show strong catalytic activity under weak acidic conditions, the effect of medium acidity on  $I_{550}/I_{450}$  was investigated in the pH range of 5.0~6.2 with HAC NaAc buffer as the medium. It can be seen from **Figure A4A** (see the supporting information in this article) that with the increase of pH, the value of  $I_{550}/I_{450}$  shows a change law of first increasing and then decreasing, and when pH = 5.4, the value of  $I_{550}/I_{450}$  is the largest. Therefore, the experiment was carried out in HAC NaAc buffer with pH = 5.4. At room temperature, the oxidation rate of OPD catalyzed by Fe, N-CQDs is slow, and the color change of the reaction system is not obvious. **Figure A4B** (see the supporting information in this article) shows the relationship between the measured I value and temperature change of Fe, N-CQDs/ $H_2O_2$ /opd mixture after incubation in a 30~60 °C water bath. It can be seen that 40 °C is a relatively suitable temperature. With the extension of the reaction time, the value of I also increases, and it is basically stable at 25 min [see the supporting information **Figure A4C**]. In order to ensure the maximum fluorescence ratio and stable signal response, 25 min is selected as the best reaction time. With the increase of OPD concentration, the  $I_{550}/I_{450}$  value gradually increases, and when the concentration is 1.75 mmol/L, the  $I_{550}/I_{450}$  value tends to be stable [see the supporting information **Figure A4D**]. The final selected experimental conditions are pH = 5.4, temperature 40 °C, reaction time 25 min, 1.75 mmol/L OPD.

### 2.4. Colorimetric/ratio fluorescence dual signal detection of $H_2O_2$ and glucose

Under the optimized conditions, the effect of  $H_2O_2$  concentration on the absorption and fluorescence spectra of the system was investigated. The results of UV-Vis absorption spectrum showed that when the concentration of  $H_2O_2$  increased from 1.0  $\mu\text{mol/L}$  increased to 300  $\mu\text{mol/L}$ , the wavelength of the characteristic absorption peak of DAP at 420 nm remains unchanged, and the absorption intensity gradually increases [see the supporting information **Figure A5A**]; and the

absorbance value ( $A_{420}$ ) at 420 nm has a good linear relationship with  $\text{H}_2\text{O}_2$  concentration [see the supporting information **Figure A5B**]. The linear equation is  $A_{420} = 0.0039c_{\text{H}_2\text{O}_2} + 0.0087$ , and the correlation coefficient is 0.996. The fluorescence measurement results show that with the increase of  $\text{H}_2\text{O}_2$  concentration, the fluorescence of DAP at 550 nm gradually increases, while the fluorescence of Fe, N-CQDs at 450 nm gradually decreases [see the supporting information **Figure A5C**]  $\text{H}_2\text{O}_2$  concentration is within the range of 1.0~80  $\mu\text{mol/L}$ , there is a good linear relationship between  $I_{550}/I_{450}$  value and  $\text{H}_2\text{O}_2$  concentration [see the supporting information **Figure A5D**], the linear equation is  $I_{550}/I_{450} = 0.0039c_{\text{H}_2\text{O}_2} + 0.2606$ , and the correlation coefficient is 0.998. Detection limit of colorimetric and ratio fluorimetry ( $3\sigma/k$ ) are respectively 0.7 and 0.6  $\mu\text{mol/L}$ , indicating that the method has high sensitivity.

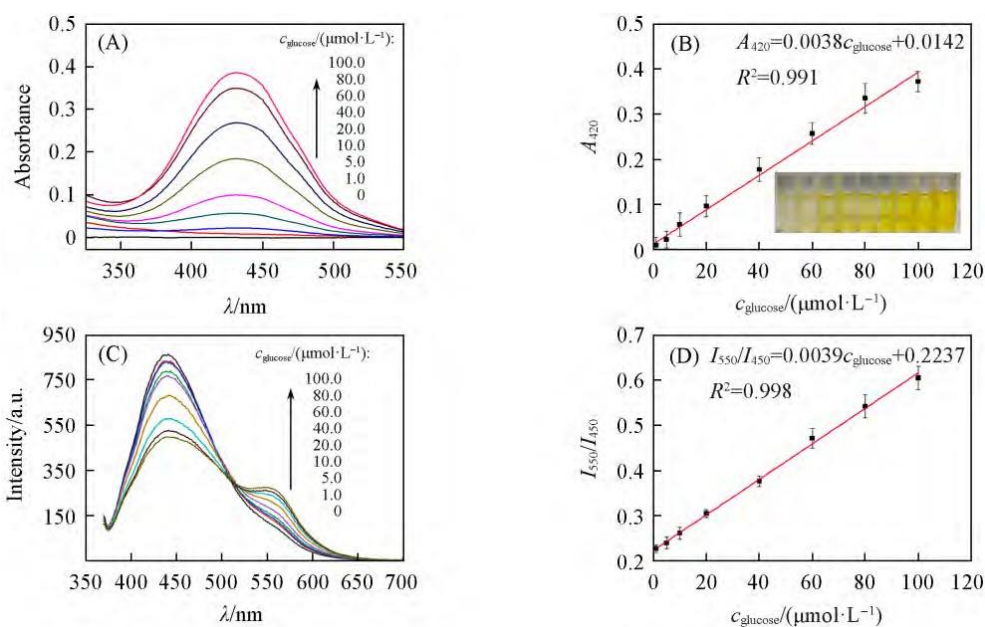


**Figure 7.** (A) Absorption; (B) and linear relationship between  $I_{550}/I_{450}$  and glucose concentration; (C) emission spectra of Fe, N-CDs-OPD with different concentrations of glucose, linear relationship between  $A_{420}$  and glucose concentration (D). Inset of (B) is the photograph of the solutions corresponding to (A).

Glucose will produce  $\text{H}_2\text{O}_2$  after catalytic oxidation by glucose oxidase. Therefore, a dual signal method for the determination of glucose can be further established. **Figure 7A** shows the absorption spectrum of DAP depending on glucose concentration. With the increase of glucose concentration, the absorbance at 420 nm gradually increased; within the concentration range of 1.0 and 100  $\mu\text{mol/L}$ , the absorbance of DAP has a good linear relationship with glucose concentration (**Figure 7B**), and the regression equation is  $A_{420} = 0.0038c_{\text{glucose}} + 0.0142$  ( $R^2 = 0.991$ ). As can be seen from **Figure 7C**, with the increase of glucose concentration, the fluorescence intensity of DAP at 550 nm increases, while the fluorescence intensity of Fe, N-CDs at 450 nm decreases; between 1.0 and 100  $\mu\text{mol/L}$  concentration,  $I_{550}/I_{450}$  value is directly proportional to glucose concentration (**Figure 7D**), and the regression equation is  $I_{550}/I_{450} = 0.0039c_{\text{glucose}} + 0.2237$  ( $R^2 =$



0.998). The detection limits of colorimetry and ratio fluorescence were respectively 0.8 and 0.6  $\mu\text{mol/L}$ , indicating that the method has high sensitivity. The linear range and detection limit of the method are superior to or comparable to the reported methods (**Table 1**); and the color of the final test solution deepens with the increase of glucose concentration (**Figure 7B** illustration), and the lowest concentration that can be distinguished by naked eyes is 5.0  $\mu\text{mol/L}$ , this method can realize the visual detection of low concentration glucose.

**Table 1.** Comparison of different methods for detecting glucose.

Method	Material	Linear range ( $\mu\text{mol}\cdot\text{L}^{-1}$ )	LOD ( $\mu\text{mol}\cdot\text{L}^{-1}$ )	Ref.
Chromatography	3-OMG	0.39–25	0.39	[4]
Electrochemical	$\text{Dy}_2(\text{MoO}_4)_3\text{-AuNPs}$	10–1000	3.33	[5]
Fluorimetry	$\text{Tm@NaYF}_4$ Nanoparticles	0–250	3.7	[12]
Fluorimetry	Co-NC	1–50	0.15	[34]
Colorimetry	$\text{mFe}_2\text{O}_3\text{-G}$	0.5–10	0.5	[35]
Colorimetry	$\text{MoS}_2$	5–150	1.2	[10]
Fluorimetry	Fe, N-CDs	1.0–100	0.6	This work
Colorimetry	Fe, N-CDs	1.0–100	0.8	This work

## 2.5. Method selectivity

To evaluate the selectivity of the method, common metal ions in serum such as  $\text{Na}^+$ ,  $\text{K}^+$ ,  $\text{Mg}^{2+}$ ,  $\text{Zn}^{2+}$  and a series of amino acids [phenylalanine (PHE)] were selected. Glycine (Gly), isoleucine (ILE), Threonine (THR), aspartic acid (ASP), tryptophan (TRP), valine (VAL) and serine (SER)] were cultivated as distractors instead of glucose. After color development, the absorption and fluorescence signals were measured respectively. **Figure 8A,B** respectively show the colorimetric and ratio fluorescence responses when the concentration of glucose (Glu) is 0.1 mmol/L and the concentration of each interfering substance is 1.0 mmol/L. Although the concentration of each interfering substance is 10 times that of glucose, only glucose can cause significant changes in the two analytical signals, which is related to the high selectivity of glucose oxidase. Therefore, the selectivity of this method is good.

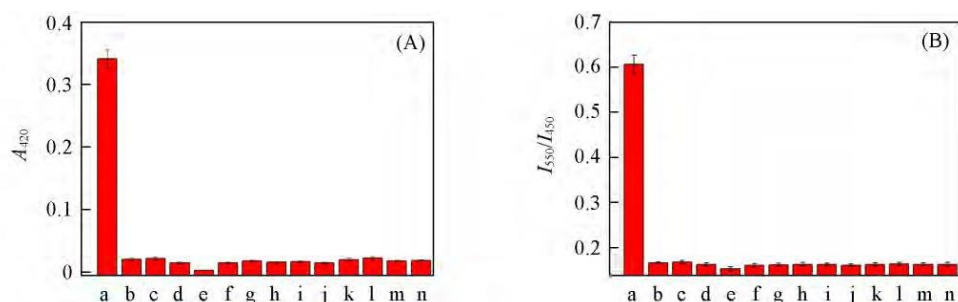


**Figure 8.** (A) selectivities of colorimetric; (B) ratio fluorescence for glucose detection.

The concentration of glucose was 0.1 mmol/L, of other substances was 1.0 mmol/L. A) Glu; b) Blank; c)  $\text{Na}^+$ ; d)  $\text{K}^+$ ; e)  $\text{Zn}^{2+}$ ; f)  $\text{Mg}^{2+}$ ; g) Phe; h) Glycine; i) Ile; j) Thr; k) Asp; l) Try; m) Val; n) Ser.

## 2.6. Actual sample analysis

In order to verify the feasibility of the method, the content of glucose in human serum was determined. Take 0.8 mL of serum sample, add 0.8 mL of trichloroacetic acid (mass fraction 5%), and centrifuge for 10 min at the speed of 10,000 r/min to remove serum protein. Add 0.1 mL of treated serum and different concentrations of glucose to the reaction system, and determine according to the steps in Section 1.3. The results are shown in **Table 2**. The colorimetric values of glucose concentration in the sample detection solution were respectively 40.2 and 35.9  $\mu\text{mol/L}$ , according to the dilution ratio, the concentration of glucose in the original sample is calculated to be 4.02 and 3.59 mmol/L respectively, which is basically consistent with the clinical measurement results (4.53 and 3.86 mmol/L), both within the normal range. In addition, the results of colorimetry and ratio fluorescence are consistent; the recovery rate is 93.3%–111.5%; the RSD is between 0.4% and 6.8%, indicating that the method has high accuracy and precision, and can be applied to the analysis of actual samples.

**Table 2.** Detection of glucose in human serum\*.

Sample	Added ( $\mu\text{mol}\cdot\text{L}^{-1}$ )	Colorimetric (%)			Ratiometric fluorescence		
		Found/( $\mu\text{mol}\cdot\text{L}^{-1}$ )	Recovery (%)	RSD ( $n = 3$ , %)	Found ( $\mu\text{mol}\cdot\text{L}^{-1}$ )	Recovery (%)	RSD ( $n = 3$ , %)
Serum 1	0	40.2	-	1.5	39.1	-	0.4
	20	61.5	106.5	2.9	61.4	111.5	3.0
	40	82.3	105.2	3.7	80.0	102.2	3.1
Serum 2	0	35.9	-	3.3	35.3	-	2.1
	20	57.6	108.5	1.4	55.2	99.5	4.6
	40	78.3	106.0	5.2	72.6	93.3	6.8

\* The serum was diluted 100 times.

## 3. Conclusion

Take biomass (leaves of syncarpic taro). Bifunctional Fe, N-CDs with peroxidase like activity and fluorescence characteristics were prepared from iron and nitrogen-containing substances. After adding  $\text{H}_2\text{O}_2$  to the mixed solution of Fe, N-CDs and OPD, Fe, N-CDs can catalyze  $\text{H}_2\text{O}_2$  to oxidize OPD to produce DAP that can emit fluorescence. DAP and Fe, N-CDs form a double emission system. The relative fluorescence intensity of the system and the absorbance of DAP are regulated by the concentration of  $\text{H}_2\text{O}_2$ . Based on the principle that glucose oxidase catalyzes the oxidation of glucose to produce  $\text{H}_2\text{O}_2$ , a colorimetric/ratio fluorescence dual signal analytical method for the determination of glucose was developed. This method has high sensitivity. It has been applied to the determination of glucose in human serum, and the results are consistent with the clinical values. Compared with the reported double signal glucose determination method, this method only needs to prepare a nano material.

**Author contributions:** Conceptualization, C.Y. and Y.X.; formal analysis, X.Y.; Y.W. and R.S.; investigation, Y.W.; writing—original draft preparation, S.C., X.Q.

and S.C.; funding acquisition, X.Q. All authors have read and agreed to the published version of the manuscript.

**Funding:** National Natural Science Foundation of China (approval No.: 61664002) and Guangxi Graduate Education Innovation Program (approval No.: Ycsw2020016).

**Conflict of interest:** The authors declare no conflict of interest.

## References

1. Zhang J, Dai X, Song ZL, et al. One-pot enzyme- and indicator-free colorimetric sensing of glucose based on MnO<sub>2</sub> nano-oxidizer. *Sensors and Actuators B: Chemical*. 2020; 304: 127304. doi: 10.1016/j.snb.2019.127304
2. Baek SH, Roh J, Park CY, et al. Cu-nanoflower decorated gold nanoparticles-graphene oxide nanofiber as electrochemical biosensor for glucose detection. *Materials Science and Engineering: C*. 2020; 107: 110273. doi: 10.1016/j.msec.2019.110273
3. Xie WQ, Gong YX, Yu KX. Rapid quantitative detection of glucose content in glucose injection by reaction headspace gas chromatography. *J. Chromatogr. A*. 2017; 1520143-1520146.
4. Ling Z, Xu P, Zhong Z, et al. Sensitive determination of glucose in Dulbecco's modified Eagle medium by high-performance liquid chromatography with 1-phenyl-3-methyl-5-pyrazolone derivatization: application to gluconeogenesis studies. *Biomedical Chromatography*. 2015; 30(4): 601-605. doi: 10.1002/bmc.3589
5. Huang HP, Yue YF, Xu L, et al. Glucose Biosensor Based on Dy<sub>2</sub>(MoO<sub>4</sub>)<sub>3</sub>-AuNPs Composite Nanomaterial<sup>†</sup>. *Chem. J. Chinese Universities*. 2017; 38(4): 554-560.
6. Xu L, Lin YQ, Chen X, et al. Electrodeposition of Platinum Nanoparticles on MgAl-layered Double Hydroxide Modified Indium Tin Oxide Electrode for Electrochemical Glucose Biosensor<sup>†</sup>. *Chem. J. Chinese Universities*. 2016; 37(3): 442-447.
7. Liu T, Zhang S, Liu W, et al. Smartphone based platform for ratiometric fluorometric and colorimetric determination H<sub>2</sub>O<sub>2</sub> and glucose. *Sensors and Actuators B: Chemical*. 2020; 305: 127524. doi: 10.1016/j.snb.2019.127524
8. Rashtbari S, Dehghan G, Amini M. An ultrasensitive label-free colorimetric biosensor for the detection of glucose based on glucose oxidase-like activity of nanolayered manganese-calcium oxide. *Analytica Chimica Acta*. 2020; 1110: 98-108. doi: 10.1016/j.aca.2020.03.021
9. Cheng X, Huang L, Yang X, et al. Rational design of a stable peroxidase mimic for colorimetric detection of H<sub>2</sub>O<sub>2</sub> and glucose: A synergistic CeO<sub>2</sub>/Zeolite Y nanocomposite. *Journal of Colloid and Interface Science*. 2019; 535: 425-435. doi: 10.1016/j.jcis.2018.09.101
10. Lin T, Zhong L, Guo L, et al. Seeing diabetes: visual detection of glucose based on the intrinsic peroxidase-like activity of MoS<sub>2</sub> nanosheets. *Nanoscale*. 2014; 6(20): 11856-11862. doi: 10.1039/c4nr03393k
11. Liu H, Hua Y, Cai Y, et al. Mineralizing gold-silver bimetal into hemin-melamine matrix: A nanocomposite nanozyme for visual colorimetric analysis of H<sub>2</sub>O<sub>2</sub> and glucose. *Analytica Chimica Acta*. 2019; 1092: 57-65. doi: 10.1016/j.aca.2019.09.025
12. Yuan J, Cen Y, Kong XJ, et al. MnO<sub>2</sub>-Nanosheet-Modified Upconversion Nanosystem for Sensitive Turn-On Fluorescence Detection of H<sub>2</sub>O<sub>2</sub> and Glucose in Blood. *ACS Applied Materials & Interfaces*. 2015; 7(19): 10548-10555. doi: 10.1021/acsami.5b02188
13. Wang HB, Chen Y, Li N, et al. A fluorescent glucose bioassay based on the hydrogen peroxide-induced decomposition of a quencher system composed of MnO<sub>2</sub> nanosheets and copper nanoclusters. *Microchimica Acta*. 2016; 184(2): 515-523. doi: 10.1007/s00604-016-2045-7
14. Xiao N, Liu SG, Mo S, et al. B,N-carbon dots-based ratiometric fluorescent and colorimetric dual-readout sensor for H<sub>2</sub>O<sub>2</sub> and H<sub>2</sub>O<sub>2</sub>-involved metabolites detection using ZnFe<sub>2</sub>O<sub>4</sub> magnetic microspheres as peroxidase mimics. *Sensors and Actuators B: Chemical*. 2018; 273: 1735-1743. doi: 10.1016/j.snb.2018.07.097
15. Zhang W, Li X, Xu X, et al. Pd nanoparticle-decorated graphitic C<sub>3</sub>N<sub>4</sub> nanosheets with bifunctional peroxidase mimicking and ON-OFF fluorescence enable naked-eye and fluorescent dual-readout sensing of glucose. *Journal of Materials Chemistry B*. 2019; 7(2): 233-239. doi: 10.1039/c8tb02110d

16. Wang C, Tan R, Li L, et al. Dual-modal Colorimetric and Fluorometric Method for Glucose Detection Using MnO<sub>2</sub> Sheets and Carbon Quantum Dots. *Chemical Research in Chinese Universities*. 2019; 35(5): 767-774. doi: 10.1007/s40242-019-9130-5
17. Zhong QM, Huang XH, Qin QM, et al. Determination of Glucose Based on Carbon Quantum Dots as Peroxidase Mimetic Enzyme. *Chinese J. Anal. Chem.* 2018; 46(7): 1062-1068.
18. Geng X, Sun Y, Li Z, et al. Retrosynthesis of Tunable Fluorescent Carbon Dots for Precise Long-Term Mitochondrial Tracking. *Small*. 2019; 15(48). doi: 10.1002/smll.201901517
19. Guo S, Sun Y, Geng X, et al. Intrinsic lysosomal targeting fluorescent carbon dots with ultrastability for long-term lysosome imaging. *Journal of Materials Chemistry B*. 2020; 8(4): 736-742. doi: 10.1039/c9tb02043h
20. Chen Y, Qin X, Yuan C, et al. Double responsive analysis of carbaryl pesticide based on carbon quantum dots and Au nanoparticles. *Dyes and Pigments*. 2020; 181: 108529. doi: 10.1016/j.dyepig.2020.108529
21. Su A, Wang D, Shu X, et al. Synthesis of Fluorescent Carbon Quantum Dots from Dried Lemon Peel for Determination of Carmine in Drinks. *Chemical Research in Chinese Universities*. 2018; 34(2): 164-168. doi: 10.1007/s40242-018-7286-z
22. Yuan C, Qin X, Xu Y, et al. High sensitivity detection of H<sub>2</sub>O<sub>2</sub> and glucose based on carbon quantum dots-catalyzed 3,3',5,5'-tetramethylbenzidine oxidation. *Microchemical Journal*. 2020; 159: 105365. doi: 10.1016/j.microc.2020.105365
23. Yadav PK, Singh VK, Chandra S, et al. Green Synthesis of Fluorescent Carbon Quantum Dots from *Azadirachta indica* Leaves and Their Peroxidase-Mimetic Activity for the Detection of H<sub>2</sub>O<sub>2</sub> and Ascorbic Acid in Common Fresh Fruits. *ACS Biomaterials Science & Engineering*. 2018; 5(2): 623-632. doi: 10.1021/acsbiomaterials.8b01528
24. Chandra S, Singh VK, Yadav PK, et al. Mustard seeds derived fluorescent carbon quantum dots and their peroxidase-like activity for colorimetric detection of H<sub>2</sub>O<sub>2</sub> and ascorbic acid in a real sample. *Analytica Chimica Acta*. 2019; 1054: 145-156. doi: 10.1016/j.aca.2018.12.024
25. Wang L, Liu Y, Yang Z, et al. A ratiometric fluorescence and colorimetric dual-mode assay for H<sub>2</sub>O<sub>2</sub> and xanthine based on Fe, N co-doped carbon dots. *Dyes and Pigments*. 2020; 180: 108486. doi: 10.1016/j.dyepig.2020.108486
26. Zhuo S, Guan Y, Li H, et al. Facile fabrication of fluorescent Fe-doped carbon quantum dots for dopamine sensing and bioimaging application. *The Analyst*. 2019; 144(2): 656-662. doi: 10.1039/c8an01741g
27. Hu Y, Zhang L, Li X, et al. Green Preparation of S and N Co-Doped Carbon Dots from Water Chestnut and Onion as Well as Their Use as an Off-On Fluorescent Probe for the Quantification and Imaging of Coenzyme A. *ACS Sustainable Chemistry & Engineering*. 2017; 5(6): 4992-5000. doi: 10.1021/acssuschemeng.7b00393
28. Sun X, He J, Yang S, et al. Green synthesis of carbon dots originated from *Lycii Fructus* for effective fluorescent sensing of ferric ion and multicolor cell imaging. *Journal of Photochemistry and Photobiology B: Biology*. 2017; 175: 219-225. doi: 10.1016/j.jphotobiol.2017.08.035
29. Shen J, Shang S, Chen X, et al. Facile synthesis of fluorescence carbon dots from sweet potato for Fe<sub>3</sub><sup>+</sup> sensing and cell imaging. *Materials Science and Engineering: C*. 2017; 76: 856-864. doi: 10.1016/j.msec.2017.03.178
30. Gu D, Shang S, Yu Q, et al. Green synthesis of nitrogen-doped carbon dots from lotus root for Hg(II) ions detection and cell imaging. *Applied Surface Science*. 2016; 390: 38-42. doi: 10.1016/j.apsusc.2016.08.012
31. Wen X, Shi L, Wen G, et al. Green synthesis of carbon nanodots from cotton for multicolor imaging, patterning, and sensing. *Sensors and Actuators B: Chemical*. 2015; 221: 769-776. doi: 10.1016/j.snb.2015.07.019
32. Yang W, Huang T, Zhao M, et al. High peroxidase-like activity of iron and nitrogen co-doped carbon dots and its application in immunosorbent assay. *Talanta*. 2017; 164: 1-6. doi: 10.1016/j.talanta.2016.10.099
33. Fang A, Long Q, Wu Q, et al. Upconversion nanosensor for sensitive fluorescence detection of Sudan I-IV based on inner filter effect. *Talanta*. 2016; 148: 129-134. doi: 10.1016/j.talanta.2015.10.048
34. Qian P, Qin Y, Lyu Y, et al. A hierarchical cobalt/carbon nanotube hybrid nanocomplex-based ratiometric fluorescent nanosensor for ultrasensitive detection of hydrogen peroxide and glucose in human serum. *Analytical and Bioanalytical Chemistry*. 2019; 411(8): 1517-1524. doi: 10.1007/s00216-019-01573-z
35. Xing Z, Tian J, Asiri AM, et al. Two-dimensional hybrid mesoporous Fe<sub>2</sub>O<sub>3</sub>-graphene nanostructures: A highly active and reusable peroxidase mimetic toward rapid, highly sensitive optical detection of glucose. *Biosensors and Bioelectronics*. 2014; 52: 452-457. doi: 10.1016/j.bios.2013.09.029

## Appendix

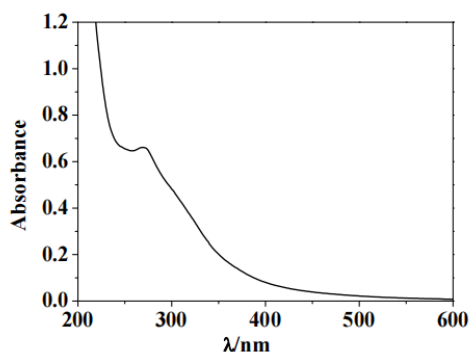


**Figure A1.** UV-vis spectra of Fe, N-CDs.

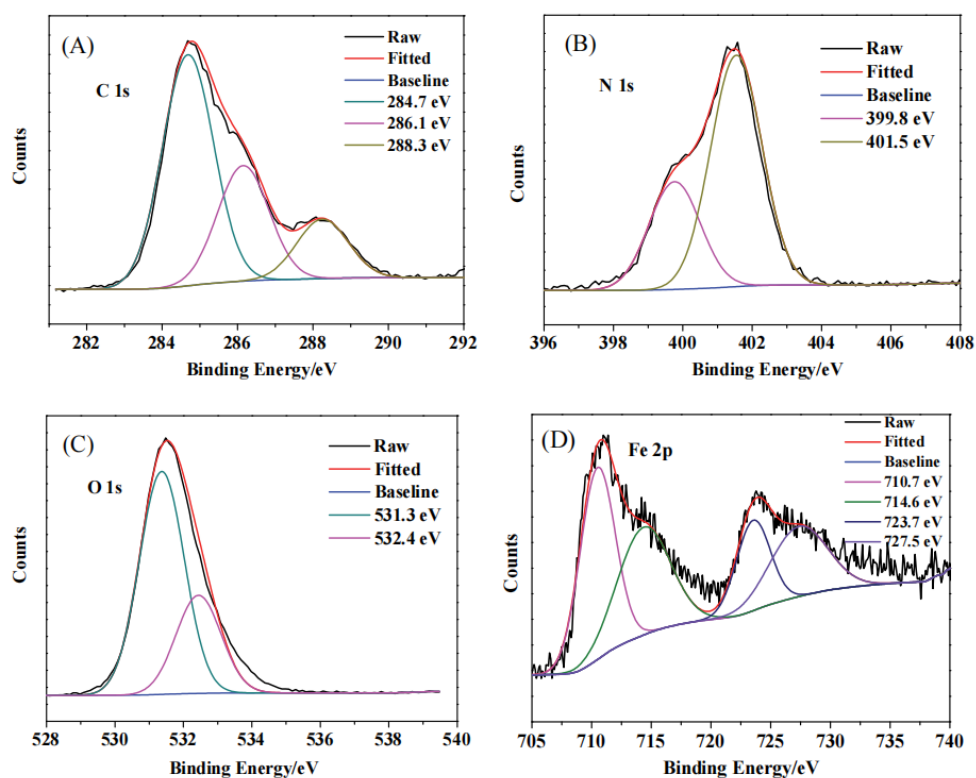


**Figure A2.** (A) C<sub>1s</sub>; (B) N<sub>1s</sub>; (C) O<sub>1s</sub>; and (D) Fe of XPS spectra of Fe, N-CDs.

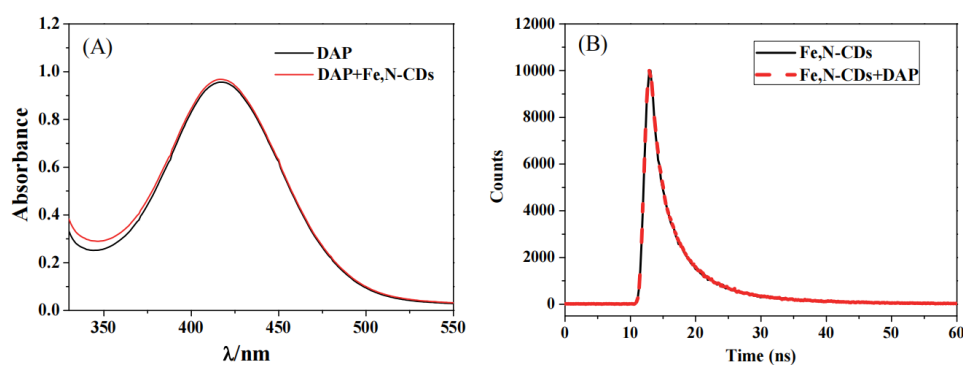


**Figure A3.** (A) Absorbance spectra of DAP in the absence and presence of Fe, N-CDs; (B) the fluorescence lifetime spectra of Fe, N-CDs in the absence and presence of DAP.

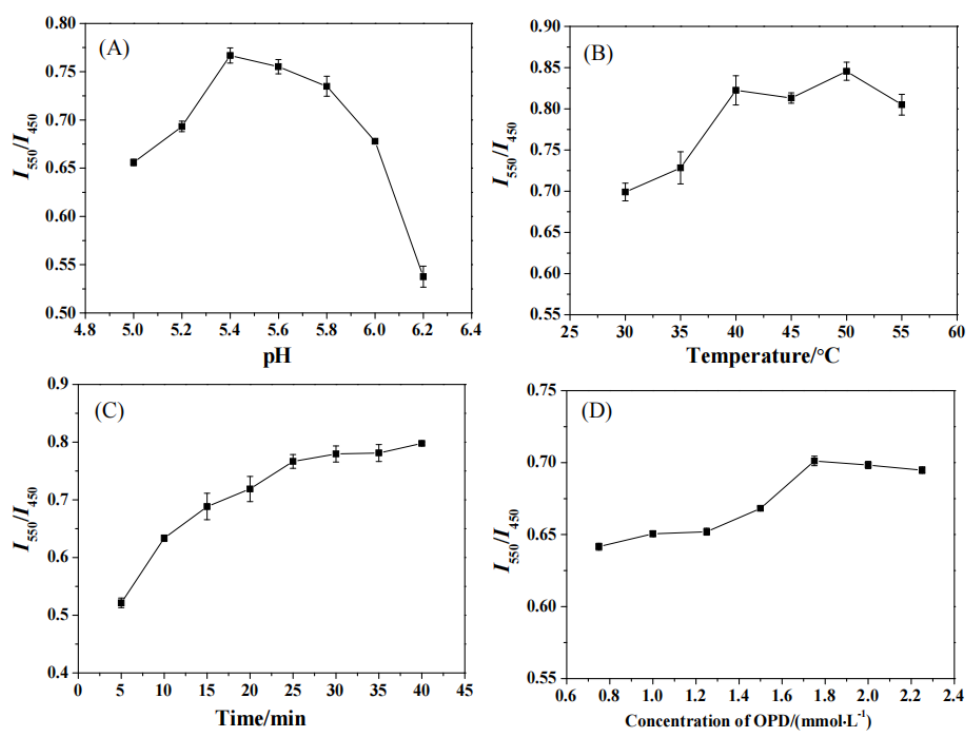


**Figure A4.** The response of the sensing system at different (A) pH; (B) temperature; (C) time; and (D) concentration of OPD.

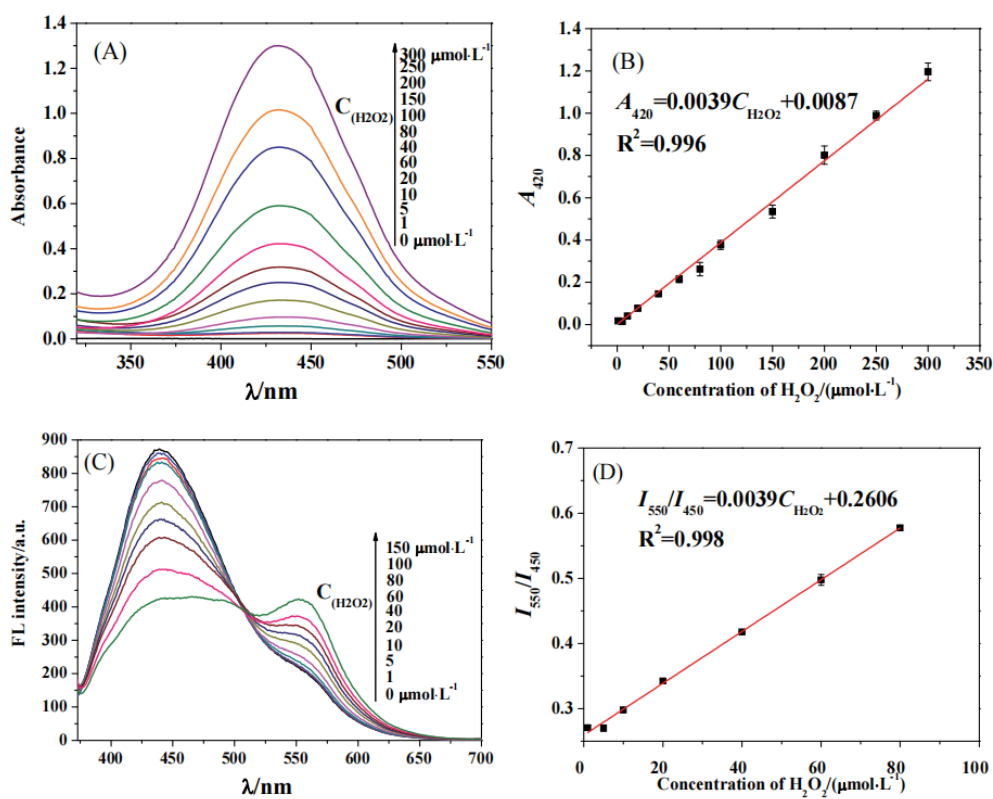


**Figure A5.** (A) Absorbance spectra of Fe, N-CDs-OPD with different concentrations of H<sub>2</sub>O<sub>2</sub>; (B) the linear relationship between  $A_{420}$  and H<sub>2</sub>O<sub>2</sub> concentration; (C) emission spectra of Fe, N-CDs-OPD with different concentrations of H<sub>2</sub>O<sub>2</sub>; (D) the linear relationship between  $I_{550}/I_{450}$  and H<sub>2</sub>O<sub>2</sub> concentration.